APPLICATION OF THE FAST CALCULATION TECHNOLOGIES TO SIMULATION OF NON-STATIONARY SUPERSONIC VISCID FLOW WITH COMBUSTION

V.V.Vlasenko*, A.A.Shiryaeva*
***Central Aerohydrodynamic Institute (TsAGI), Zhukovsky, Russia**
vlasenko.vv@yandex.ru; anja.shiryaeva@gmail.com

Keywords: *unsteady RANS, stabilization of combustion, supersonic flow*

Abstract

Fast technology for computation of non-stationary viscid flows is presented. It is based on explicit scheme with Fractional Time Stepping. For boundary layers, "wall law" boundary condition is used. Possibility of using another approach, Local Dual–Time Stepping, is discussed. Technology is applied to supersonic flow in a duct with combustion of hydrocarbon fuel in pseudoshock. High-frequency oscillations of flame front in the duct are found and analyzed. Their influence on the flame stabilization in the duct is shown. Correlation between useful force and heat release is demonstrated.

1 General Introduction

The main object of this paper is the problem of flame stabilization in a duct with supersonic flow at the entrance.

Flows of this class have multiscale character. Turbulent jets of fuel interact with shock waves and with separated boundary layers – in presence of finite-rate chemical kinetics. It is also characteristic that the combustion stabilization in a duct is preceded by a stage of non-stationary flow development with the combustion propagation along the duct. It is necessary to find numerical methods, which may provide the sufficient quality in solution of such tasks. Implicit schemes, which are widely used in simulation of viscid gas flows, are very effective in solution of stationary tasks, but demonstrate very low quality in description of non-stationary flows (especially if convective processes are essential). For high-quality description of non-stationary flow, during one time step the information should propagate to a distance that should be less than one step of computational grid (Courant-Friedrich-Levy principle, CFL). In such situation the natural choice is the use of explicit numerical schemes. But CFL-condition requires the use of very low time steps; in multiscale tasks, it results in extremely large computation time. Numerical technologies, which would improve the efficiency of explicit schemes with keeping the correct description of non-stationary phenomena, are required.

This paper presents one possible variant of such technology – Fractional Time Stepping (FTS) in combination with the "wall law" boundary condition. After that, this technology is applied to numerical simulation of supersonic flow in a duct with combustion of hydrocarbon fuel in pseudoshock. Previous results obtained by authors in simulation of such flows were published in [1] and [2]. Some data from these previous works will be supplemented here with new results.

2 Technology of computations

2.1 Equations and numerical method

Flow simulation is performed on the basis of full unsteady Reynolds equation system for multi-component compressible gas with finite-rate chemical reactions in 2D (plane) flow approximation. The equation system is closed

by $(q-\omega)$-turbulence model [3] and by a kinetic scheme of gaseous hydrocarbon fuel combustion in air. The kinetic scheme is similar to the scheme [4]; it includes one quasi–global reaction of hydrocarbon fuel decomposition into CO and H_2O and 11 reactions in H-C-O system with participation of N_2 as inert component. This simple model gives inexact description of the inner stages of reaction process, but it is adjusted to provide correct ignition delay for the range of initial temperature $T = 950...1600\ K$ and initial pressure $p = 0.1...10$ atm. Influence of turbulence on chemistry is neglected in this work, and the rates of chemical reactions are calculated using the time-averaged values of mixture parameters.

A numerical method of the 2^{nd} approximation order in all variables is used. This method includes explicit monotonic Godunov-Kolgan-Rodionov scheme for convective fluxes, explicit modified central-difference approximation of diffusive terms and local implicit approximation of source terms. Detailed description of various elements of this numerical method can be found in works [5-7]. Multi-block regular grids are used in calculations.

2.2 Fast technology for computation of unsteady viscid flows

This paper presents results obtained using the technology for fast and correct simulation of unsteady viscid flows that has been published in [1,2]. It consists of two main elements: 1) Fractional Time Stepping (FTS); 2) "wall law" boundary condition at no-slip solid walls.

The calculations are performed on strongly non-uniform grids with compression to solid walls. The maximal value of time step, which is necessary for stability of explicit scheme in various grid cells, can differ by several orders of magnitude. The FTS technology allows to accelerate the calculation. [8] is the first work, where this technology was applied to the calculation of flows with combustion. Here the original variant of FTS technology is used; it was previously described in [6].

The calculation is performed with different time step in different grid cells. In each separate cell, the value of time step is taken to be equal to $\tau = \tau_{\max} / 2^k$, where $\tau_{\max}$ is the maximal value of time step in the whole computational domain and the integer parameter k is chosen to satisfy the local stability condition in the given cell. During one global time step, 2^k local time steps are performed in the current cell. The quantity of local time steps is different in different cells. However, to the end of global time step, time increases by the same value $\tau_{\max}$ in all the cells. In addition, during the intermediate local time steps, the processes in the cells with different τ are synchronized by linear interpolation in time. As a result, non–stationary flow development is described correctly.

Depending upon ratio of maximal and minimal time steps and upon the quantities of cells with different values of time step, the FTS technology can provide acceleration from several times and up to several tens times.

However, the FTS technology doesn't allow to get the reasonable CPU time, if the flow with turbulent boundary layers is simulated. If the usual no-slip boundary condition is imposed on the solid walls, the grid should resolve the main elements of the near-wall part of turbulent boundary layer – the viscid sublayer (which defines the friction force and the wall heat flux) and the buffer zone (where the main production of turbulence takes place). But the thickness of viscid sublayer is about 0.1% of the total thickness of boundary layer. To resolve processes in viscid sublayer, it is necessary to place 5-10 cells inside. As a result, the size of the near-wall cell should be about 0.01% of the boundary layer thickness. In this case, the stability condition in the near–wall cells appears to be so strong that the main part of work is accomplished in the deep of boundary layers. In such situation, FTS acceleration in larger cells cannot provide real acceleration of the whole computation.

To avoid this problem, the "wall law" boundary condition is applied at the no-slip solid walls. This is original variant of widely used wall function approach (another variants of this approach can be found e.g. in works

[9-11]). It allows to use grids with essentially larger near–wall cells. Typical size of near–wall cells is about 1% of the boundary layer thickness. In the "wall law" condition, it is assumed that the flow in small vicinity of the solid walls can be described by the same self-similar solution as the flow in the turbulent boundary layer on a flat plate. In particular, the dependence of tangential velocity V_τ upon the distance from the wall y may be presented in non-dimensional form $u^+ = f(y^+)$ ($u^+ = V_\tau / u_\tau$, $y^+ = y / l_\tau$, $u_\tau = \sqrt{\tau_W / \rho_W}$, $l_\tau = \nu_W / u_\tau$, where τ is tangential viscid stress, ρ is density, ν is kinematic molecular viscosity and index "W" corresponds to the values on the wall.) Substituting parameters from the center of near-wall cell into this dependence, one may find the tangential viscid stress on the wall - τ_W.

The dynamic heat exchange is assumed: wall temperature T_W varies both in time and along the wall surface. Quasi-equilibrium approximation is used. Temperature from the other side of the wall T_{out} is given, and it is assumed that each moment the heat flux q_W becomes constant across the wall. T_W and q_W are determined from the equation

$$q_W \approx \lambda\left(\frac{T_{out}+T_W}{2}\right)\cdot\frac{T_W - T_{out}}{\Delta} \approx \frac{c_p\left(T_1 - T_W\right)}{\mathrm{Pr}\cdot|V_{\tau 1}|}\cdot|\tau_W|,$$

where $\lambda(T)$ is heat conductivity of the wall, Δ is the wall width, c_p is the gas specific heat and index "1" corresponds to parameters in the center of near-wall cell.

In the same way, the diffusive flux of any parameter at the solid wall may be expressed through τ_W. Adding the wall pressure $p_W \approx p_1$ to these diffusive fluxes, one may calculate the whole fluxes of all parameters at the wall and to substitute them into balance equations for the near-wall cell. Important original feature of the presented here "wall law" boundary condition is the use of self-similar profiles of source terms for turbulence parameters in the balance equations for near-wall cell. Details of this boundary condition may be found in [2].

For testing this numerical technology, the test task about propagation of strong shock wave along a duct with no-slip solid walls (without combustion) was considered in [1,2]. Calculations were performed on two grids. First grid was constructed for the use of no-slip boundary condition; it contained 20 cells across the boundary layers with $y^+ \sim 1$ for the centers of near-wall cells. Calculation on such grid with standard approach for explicit scheme (global time stepping - GTS: equal time step in all cells; the value of time step is determined by the strongest stability restriction) required 27.5 hours of CPU time. Application of FTS technology allowed to diminish the time of computation 15 times; however, analogous calculation for multi-component gas with finite-rate combustion would be too long. After that, the second grid was considered. It was constructed for the use of "wall law" boundary condition; it contained 10 cells across the boundary layers with $y^+ \sim 100$ for the centers of near-wall cells. Calculation with global time stepping on this grid was 50 times faster then on the previous grid; application of FTS technology allowed to accelerate calculation 4 times more, providing total acceleration nearly 200 times. The worsening of the numerical solution in comparison with GTS computation on the first grid was acceptable: errors in distributions of all parameters were about several percents. This result was obtained for strong shock-boundary layer interactions, with formation of large boundary layer separations.

To improve the accuracy of calculations, in the nearest future it is supposed to apply another fast numerical technology - Local Dual-Time Stepping. In this case, no-slip boundary condition will be imposed at the solid walls, and appropriate grid will be used. In the cells, where the effect of FTS technology is insufficient (where the time step is more than $2^{11} - 2^{12}$ times lower than the maximal time step), the calculation will be performed using non-linear implicit scheme with 2nd accuracy order in time with the well-known dual-time stepping procedure (see e.g. [12]). In the rest part of computational domain, the explicit scheme with FTS technology will be applied.

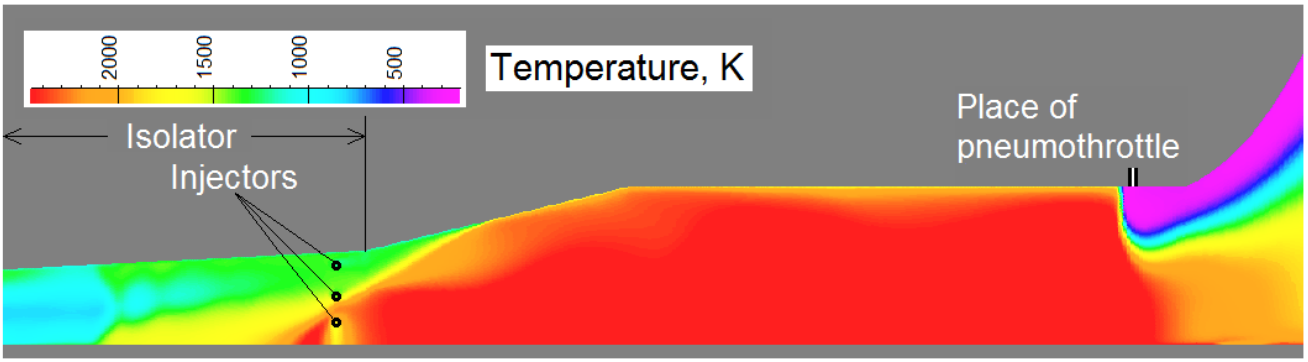

Fig. 1. Geometry of the duct and typical flow structure during throttling ($\alpha = 1.2$).
The picture is stretched in vertical direction.

3 Calculations of supersonic viscid flow with combustion in a flat duct

3.1 Geometry and flow regime

Fast technology, based on combination of FTS with the "wall law" boundary condition, has been applied to numerical simulation of combustion in a flat duct with supersonic flow at the entrance (Fig.1). The duct includes: "isolator" with slow expansion along the longitudinal axis x; the part with strong expansion of the duct and the part with constant width. At the right end of duct, the supersonic nozzle begins; it is not shown in pictures. Air flow with $M \approx 2.5$, $T \approx 800\ K$ at the duct axis and with thick boundary layers (50% and 30% of the duct width) enters through the left end of the duct. Three injectors of hydrocarbon fuel are placed just before the right end of isolator (their positions are shown in Fig.1). Fuel is injected perpendicular to flow (in direction of z axis); injection is simulated in 2D computation in the plane $(x; y)$ as local sources of the fuel mass, of energy and of turbulence.

Computational grid contains 46 cells across the duct (with $y^+ \sim 10$ in the centers of first near-wall cells). Lower wall of the duct was considered as heat-insulated (heat flux on the wall $q_W = 0$). At the upper wall, quasi-equilibrium dynamic heat exchange was simulated; temperature of the wall outer surface (from the other side of the wall) $T_{out} \approx 420\ K$.

Calculation shows that the injected fuel doesn't self-ignite. To obtain combustion in the duct, a pneumothrottle is placed on the upper wall, just before the right end of duct (Fig.1). It produces the perpendicular-to-wall jet of high-pressure air. It leads to choking of the duct and to formation of a pseudoshock - region of flow, where the transition from supersonic to subsonic flow is realized through a series of oblique shocks, which interact strongly with separated boundary layers. Burning arises in separation zones, and the flow structure, which is shown in Fig.1, is established. This structure is not stationary; flame front oscillates in longitudinal direction. After that, the pneumothrottle is switched off. This method of throttling has been repeatedly successfully tested in research investigations, held in TsAGI.

3.2 Longitudinal oscillations of flame front

For flow regimes with the integral air excess ratio $\alpha = 0.59...1.45$, stabilization of flame has been achieved after the throttling. It may be seen on the plots of integral useful longitudinal force (Fig.2). In the cases with $\alpha = 1.2$ and $\alpha = 1.45$, useful force finally becomes practically constant. Fig.3 shows typical flow structure after the flame stabilization.

However, it was found that in regimes $\alpha = 0.59$, $\alpha = 0.72$ and $\alpha = 1.02$ the stabilized flame oscillates periodically in longitudinal direction with frequency 250-300 Hz. In Fig.2, corresponding oscillations of useful force are seen.

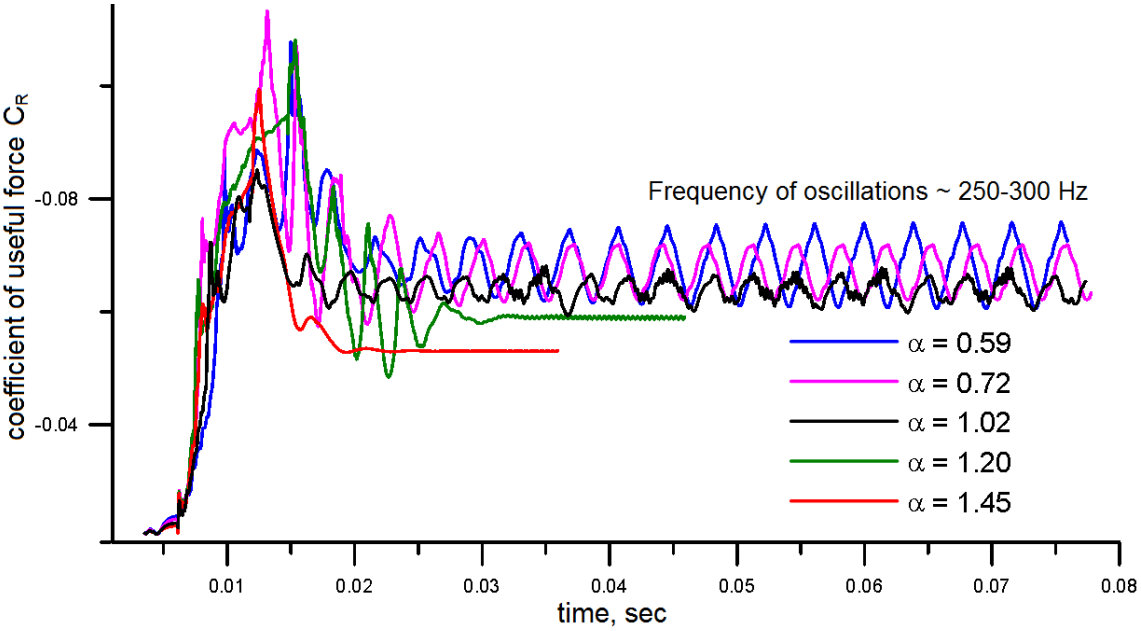

Fig. 2. Dependencies of the coefficient of integral useful force

Analysis of sequential fields of longitudinal velocity u (Fig.4) allows to explain these oscillations. Note that each field in Fig.4 contains the isoline $u = 0$. It allows to find the places of flow separation and re-attachment and to estimate the size of recirculation zone.

It was found that the main role in the flame oscillations is played by a large separation bubble that is formed in the pseudoshock structure at the lower wall. It may be seen both in Fig.3 and in Fig.4,a. The separation starts near the fuel injectors and closes after the end of the duct expansion. Above this bubble, there is supersonic flow that is gradually decelerated in a series of shocks that are poorly resolved by the grid. After the end of the duct expansion, the flow becomes fully subsonic over the whole cross-section of duct. The flow stays subsonic till the beginning of nozzle.

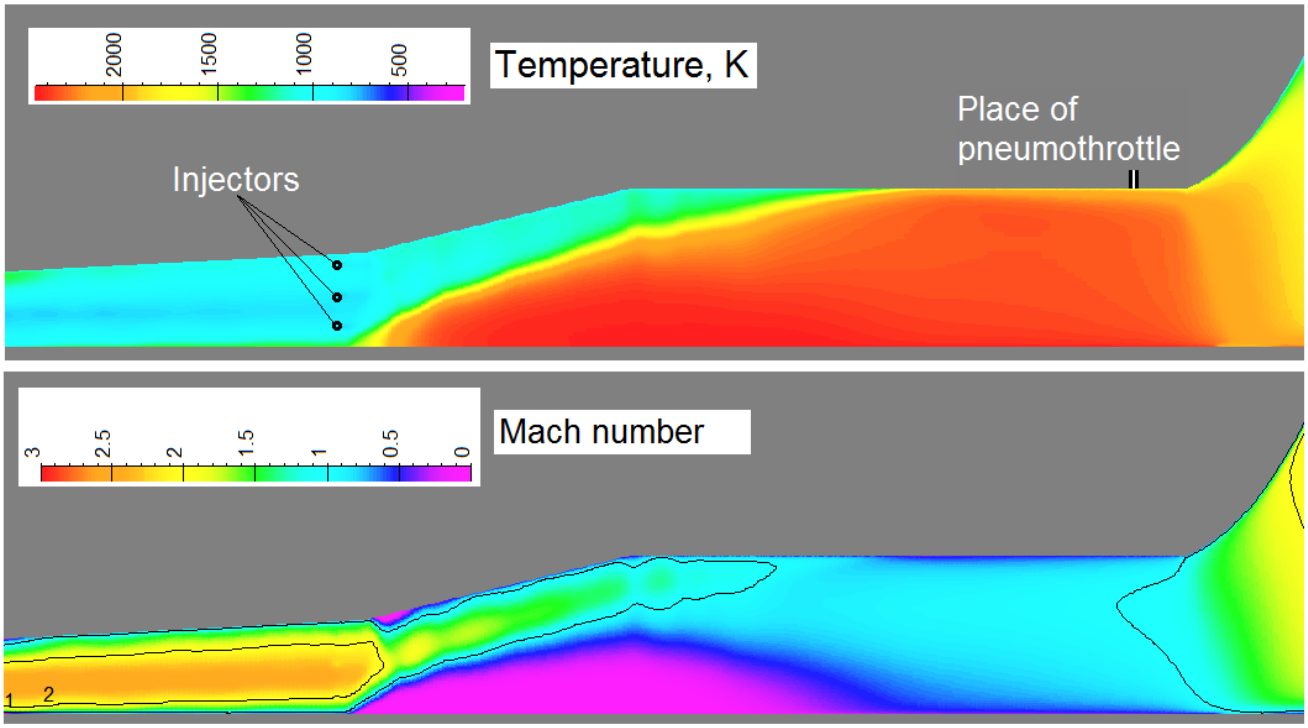

Fig. 3. Structure of flowfield in the duct after the flame stabilization ($\alpha = 1.2$)

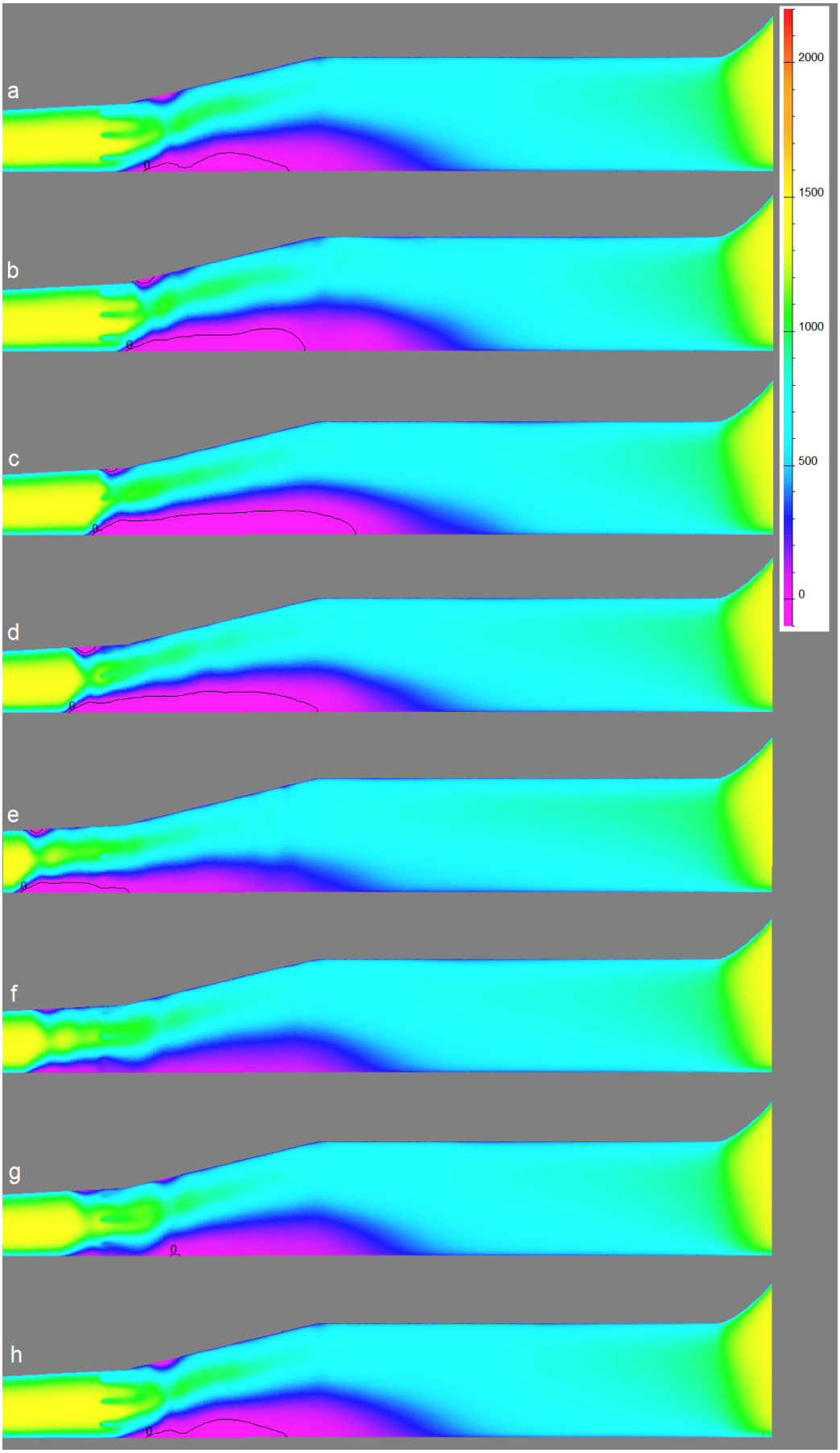

Fig. 4. Sequential fields of longitudinal velocity u [m/sec] after the flame stabilization ($\alpha = 0.6$)

In the moment, which is shown in Fig.4,a, there is no combustion in the separation bubble. Fresh fuel flows inside the bubble. Temperature here is about 2200 K, the time of the fuel residence inside the bubble is long, and in Fig.4,b the combustion begins. As a result, the volume of separation bubble begins to grow. Cross-section of supersonic stream diminishes; it leads to increase of pressure in supersonic part, and shocks shift upstream. As a result, the whole pseudoshock shifts to the left – Fig.4,c.

In Fig.4,d the combustion inside the bubble is already finished and the bubble volume begins to decrease. But the bubble interacts with the lower injector and the fresh fuel begins to flow upstream from the injector into the recirculation zone. It results in following upstream shift of the pseudoshock.

In Fig.4,e one can see the extreme left position of pseudoshock. Recirculation zone is shifted upstream from the injector and its supply by fresh fuel is stopped. Downstream from the injectors the boundary layer is attached to wall. Hot combustion products begin to move downstream. As a result, the pseudoshock finally begins to move downstream, too. In Fig.4,f one can see that recirculation zone is disappeared and the flow is directed to the right everywhere.

In Fig.4,g the formation of the new separation can be seen – downstream from the injectors. It is related with the fact that pseudoshock gradually moves downstream, velocity of supersonic flow after injection section increases and intensity of oblique shocks above the point of new separation becomes sufficient to separate the flow.

Finally, in Fig.4,h the flow structure returns to the same state as in Fig.4,a. After that the next oscillation begins.

Decrease of the oscillations amplitude with the growth of α (Fig.2) is explained by the fact that the amount of fuel diminishes, and higher and higher part of fuel is burnt in the slow flow above the recirculation zone, and the smaller and smaller part of fuel penetrates inside this zone. As a result, heat release inside the bubble diminishes, variations of its volume become smaller, and the pseudoshock oscillations degenerate gradually. It proves that the oscillations of the pseudoshock are not related with acoustic perturbations, but are produced by variation of the separation bubble volume because of the heat release inside the bubble.

3.3 Correlation between the useful force and the heat release in the duct

Let us consider the stationary flowfield in the duct. (If the stabilized flame oscillates in longitudinal direction, it is necessary to average the flowfield over the period of oscillations.) On the basis of this field, the streamlines are plotted. The quantity of heat, which is released per unit mass along the streamline due to chemical reactions between the section $x = x_0$ and the nozzle exit section $x = x_{exit}$, may be calculated by the formula:

$$q = -\sum_{k=1}^{N_{sp}} \int_{x_0}^{x_{exit}} h_k dY_k \,. \qquad (1)$$

Here N_{sp} is the quantity of chemical species, Y_k are their mass fractions and $h_k(T)$ are their enthalpies per unit mass. Integration in (1) should be performed along the streamline. After that, the total quantity of heat, that is released per unit mass between these sections in the whole duct, is calculated as follows:

$$Q = -\int_{F_{exit}} q \rho u dF \,. \qquad (2)$$

In formula (2) u is longitudinal velocity, dF is area element in the exit cross-section and q is the value (1) calculated for the streamline that passes through the current area element dF. It should be noted that formula (1) contains not only heat effect of chemical reactions, but also spatial redistribution of heat due to molecular and turbulent diffusion. However, integration over the area of cross-section in (2) eliminates the contribution of diffusion.

Maximal possible heat release per unit mass $Q_{\max}$ for the given air excess ratio α may be estimated as

$$Q_{\max}(\alpha) = \frac{G_f H_{u0} \min(1;\alpha)}{1 + \alpha L_0},$$

where H_{u0} is the fuel heat capacity at standard temperature T_0 and L_0 is mass of air that is burned simultaneously with burning of 1 kg of fuel. Figure 5 presents the dependence of non-dimensional heat release $\overline{Q}(\alpha) = Q(\alpha)/Q_{\max}(1)$, obtained in calculations. For comparison, the ideal dependence $\overline{Q}_{\max}(\alpha) = Q_{\max}(\alpha)/Q_{\max}(1)$ is also shown. Discrepancy between these two curves is caused by incompleteness of combustion. Contrary to ideal curve, heat release in the duct diminishes monotonically with growth of α, because the smaller and smaller part of fuel is burned inside the recirculation zone (where the conditions for burning are very good), and the higher and higher part is burned in the direct flow in the duct (where the conditions for burning are bad).

At the same Figure, dependence of the useful force R upon α is also shown. Useful force was calculated by integration of longitudinal component of force, applied to solid walls, over the whole surface of the duct and the nozzle. It is obvious that the curve $R(\alpha)$ is in good correlation with $\overline{Q}(\alpha)$.

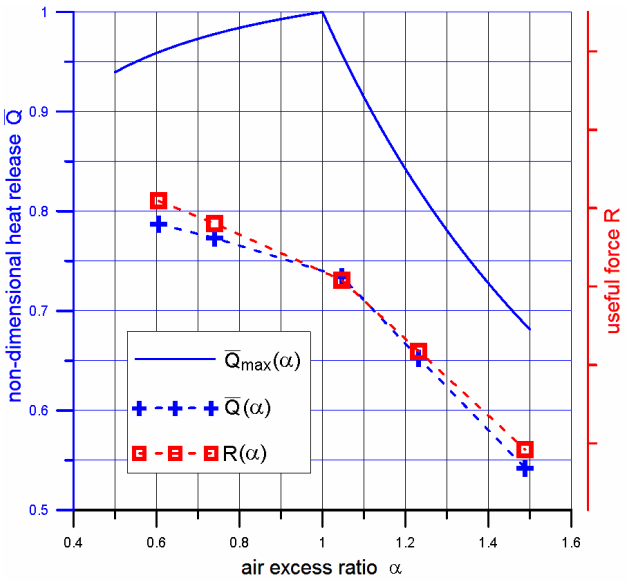

Fig. 5. Dependencies of non-dimensional heat release and useful force upon air excess ratio

3.4 One possible reason of the flameout

Calculations have shown that variation of the throttling duration may lead to the flameout. The described above mechanism of flame oscillations may explain this effect. During the throttling, the flame also oscillates in longitudinal direction. When the throttling is stopped, the rarefaction wave begins to propagate from the end of duct in upstream direction. If it reaches the pseudoshock at the moment, when the recirculation zone disappears (like at Fig.4,f), then the rarefaction diminishes the pressure in pseudoshock structure and prevents the flow from the new separation. But without the separation, the combustion is impossible, because the time of gas presence inside the duct is too small.

To exclude the flameout, it is necessary to choose the correct moment for the end of throttling. Rarefaction wave should come to pseudoshock in the moment with fully developed separation bubble.

3.5 Flow structure in the duct with narrow part

Another way to exclude the flameout is to use constant throttling of the duct. For this purpose, it is possible to diminish the duct width near the nozzle beginning. To estimate the effect of such narrowing without the optimization of its geometry, the sinusoidal narrowing was considered (Fig.6). In this case, pneumothrottle was not used.

It was found that diminishing of the duct width by 20% does not provide the self-ignition of combustion. When the duct width was diminished by 30%, the duct was choked, and pseudoshock has formed inside. Combustion has arisen in separation inside the pseudoshock structure. It resulted in shift of the pseudoshock to the left, inside the isolator, upstream from the injection section. Combustion develops in fully subsonic flow – see Fig.6 and compare it with Fig.3. In this case, the above mechanism of flame oscillations is absent, and flow structure appears to be stationary.

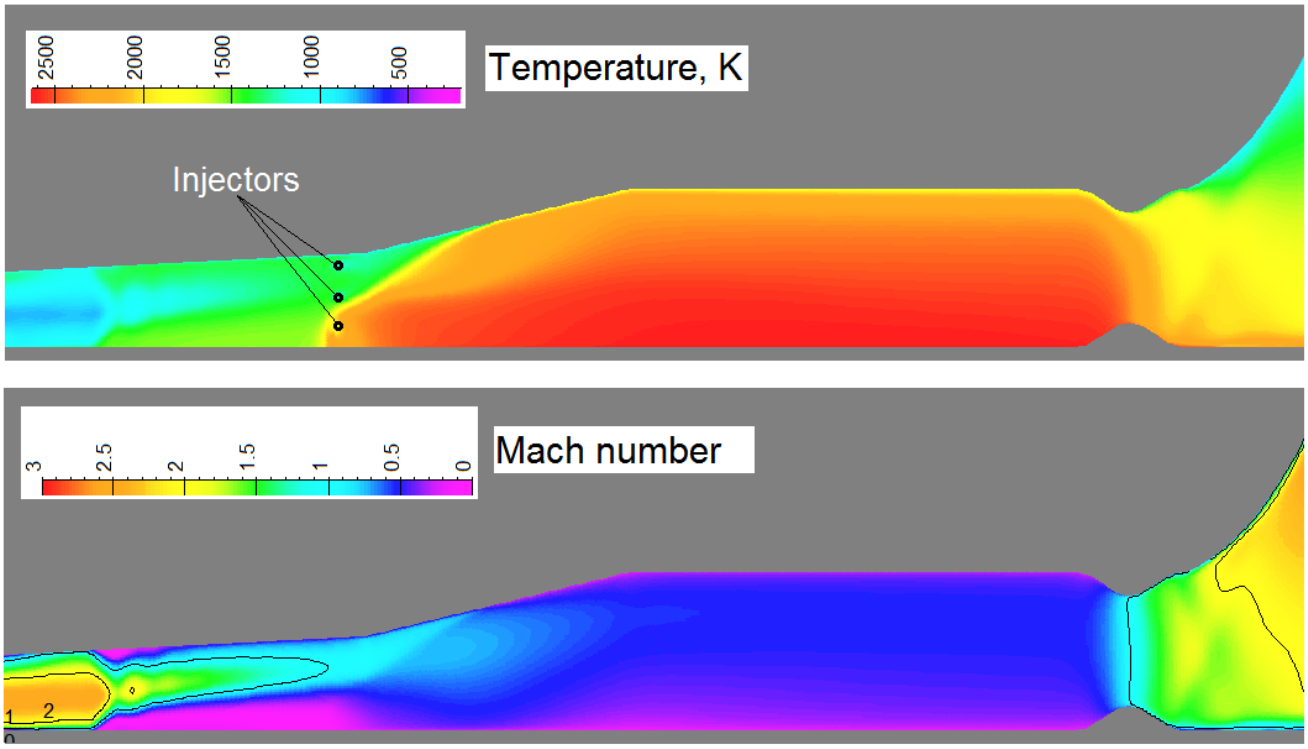

Fig. 6. Structure of flowfield after the flame stabilization for the duct with narrow part ($\alpha = 1.2$)

For the regime with $\alpha = 1.2$, the use of duct with narrow part resulted in small growth of useful force (by 5%) and in slow decrease of the combustion completeness (by 1%) in comparison with stabilized flame in the duct without narrowing.

Diminishing of the duct width by 40% resulted in choking inside the isolator with following moving of pseudoshock to the inlet.

4 Conclusions

The regimes with undamped oscillations of pseudoshock are found in computations of the flat duct with supersonic flow at the entrance. Oscillations are caused by variation of the volume of recirculation zone in pseudoshock structure. This variation is related with combustion inside the recirculation zone.

Maximal completeness of combustion is achieved at the values of the integral air excess ratio α~0.6, when the maximal quantity of fuel is burned inside the recirculation zone. Diminishing of heat release with the growth of α leads to monotonic decrease of useful longitudinal force.

Destruction of the recirculation zone in the pseudoshock structure may lead to flameout.

In the duct with narrow part the pseudoshock is placed inside the isolator, upstream from the injection section, and combustion develops in subsonic flow. Chocking of flow in isolator may lead to moving of the pseudoshock to the inlet.

5 Acknowledgement

The work was supported by Russian Foundation for Basic Research (grant 10-08-00274-a).

References

[1] Vlasenko V. Numerical simulation of the unsteady propagation of combustion in a duct with a supersonic viscous gas flow. *Russian Journal of Physical Chemistry B,* Vol. 5, No. 5, pp 800-812, 2011.

[2] Vlasenko V and Shiryaeva A. Numerical simulation of non-stationary propagation of combustion along a duct with supersonic flow of a viscid gas. *Proceedings of the Institution of Mechanical Engineers, Part G: Journal of Aerospace Engineering,* 0954410012436441, first published online on February 22, 2012.

[3] Coakley T and Hsieh T. Comparison between implicit and hybrid methods for the calculation of steady and unsteady inlet flows. *AIAA-85-1125,* 1985.

[4] Westbrook Ch and Dryer F. Chemical kinetic modeling of hydrocarbon combustion. *Prog. Energy Combust. Sci.,* Vol. 10, pp 1-57, 1984.

[5] Neyland V, Bosniakov S, Glazkov S, Ivanov A, Matyash S, Mikhailov S and Vlasenko V. Conception of electronic wind tunnel and first results of its implementation. *J. Prog. Aerosp. Sci.*, Vol. 37, pp 121-145, 2001.

[6] Bosnyakov S, Kursakov I, Lysenkov A, Matyash S, Mikhailov S and Vlasenko V. Computational tools for supporting the testing of civil aircraft configurations in wind tunnels. *J. Prog. Aerosp. Sci.*, Vol. 44, pp 67–120, 2008.

[7] Vlasenko V and Sabelnikov V. Numerical simulation of inviscid flows with hydrogen combustion after shock waves and in detonation waves. *AIAA*-94-3177, 1994.

[8] Pervaiz M and Baron J. Spatiotemporal adaptation algorithm for two-dimensional reacting flows. *AIAA Journal*, Vol. 27, No. 10, pp 1368-1376, 1989.

[9] Huang P and Coakley T. Calculations of supersonic and hypersonic flows using compressible wall functions. *NASA-TM-112910,* pp1-12, 1993.

[10] Shih T-H Povinelli L, Liu N-S and Chen K-H. Generalized wall function for complex turbulent flows. *NASA-TM-2000-209936*, pp 1-9, 2000.

[11] Nichols R and Nelson C. Wall function boundary conditions including heat transfer and compressibility. *AIAA Journal,* Vol. 42, No. 6, pp 1107-1114, 2004.

[12] Blazek J. *Computational Fluid Dynamics: Principles and Applications.* Elsevier, 2001.

Copyright Statement